EPJ Web of Conferences **60**, 20004 (2013)
DOI: 10.1051/epjconf/20136020004

Dynamics of isolated-photon plus jet production in pp collisions at $\sqrt{s} = 7$ TeV with the ATLAS detector

Josu Cantero, on behalf of the ATLAS Collaboration[1,a]

[1] *Universidad Autónoma de Madrid (UAM)*

Abstract. The dynamics of isolated-photon plus jet production in pp collisions at a centre-of-mass energy of 7 TeV has been studied with the ATLAS detector at the LHC using an integrated luminosity of 37 pb^{-1}. Measurements of isolated-photon plus jet differential cross sections are presented as functions of the photon transverse energy, the jet transverse momentum, the jet rapidity, the difference in azimuthal angle between the photon and the jet, the photon-jet invariant mass and the scattering angle in the photon-jet centre-of-mass frame. Next-to-leading-order QCD calculations are compared to the measurements and provide a good description of the data, except in the case of the azimuthal angle.

1 Introduction

The production of prompt photons in association with a jet in proton-proton collisions, $pp \rightarrow \gamma$ + jet + X, provides a testing ground for perturbative QCD (pQCD) in a cleaner environment than in jet production since the photon originates from the hard interaction and does not undergo hadronisation.

The dynamics of the underlying processes $2 \rightarrow 2$ hard collinear scattering can be investigated using the variable θ^*, $\cos\theta^* \equiv \tanh(\Delta y/2)$, where Δy is the difference in rapidity of the two final-state particles, and is sensitive to the spin of the exchanged particle. At leading order (LO) in pQCD, the process in $pp \rightarrow \gamma$ + jet + X proceeds via two production mechanims: direct photons (DP), which originate from the hard process, and fragmentation photons (F), which arise from the fragmentation of a coloured high transverse momentum, p_T, parton [1, 2]. The DP contribution is expected to exhibit a $(1 - |\cos\theta^*|)^{-1}$ dependence when $|\cos\theta^*| \rightarrow 1$, whereas that of fragmentation processes is predicted to be the same as in dijet production, namely $(1 - |\cos\theta^*|)^{-2}$. As a result, isolated-photon plus jet production provides a handle on the relative contributions of the DP and F components and the possibility to test the dominance of t-channel quark exchange.

To study the kinematics and dynamics of the isolated-photon plus jet system, measurements of the differential cross section as functions of the leading-photon transverse energy (E_T^γ), the leading-jet transverse momentum ($P_T^{\rm jet}$) and rapidity ($y^{\rm jet}$), the difference in azimuthal angle between the photon and the jet ($\Delta\phi^{\gamma j}$), the photon-jet invariant mass ($M^{\gamma j}$) and $|\cos\theta^*|$, where the variable θ^* is referred to as $\theta^{\gamma j}$ henceforth. The photon was required to be isolated by using a criterium based on the amount of transverse energy inside a cone of radius 0.4 centred around the photon. The jets were defined using the anti-k_t jet algorithm [3] with distance parameter $R = 0.6$. The measurements were performed in the phase-space region of $E_T^\gamma > 45$ GeV, $|\eta^\gamma| < 2.37$ (excluding the region of $1.37 < |\eta^\gamma| < 1.52$), $P_T^{\rm jet} > 40$ GeV, $|y^{\rm jet}| < 2.37$ and $\Delta R_{\gamma j} > 1$. The measurements of $d\sigma/dM^{\gamma j}$ and $d\sigma/d|\cos^{\gamma j}|$ were performed for $|\eta^\gamma + y^{\rm jet}| < 2.37$, $|\cos\theta^{\gamma j}| < 0.83$ and $M^{\gamma j} > 161$ GeV; these additional requirements select a region where the $M^{\gamma j}$ and $|\cos\theta^{\gamma j}|$ distributions are not distorted by the restrictions of the transverse momenta and rapidities of the photon and the jet. To gain insight into the characteristics of one of the primary backgrounds in the study of the properties of the new "Higgs-like" particle observed by ATLAS [4] and CMS [5] the measurement of $d\sigma/d|\cos\theta^{\gamma j}|$ without applying extra cuts was also performed. Next-to-leading-order (NLO) QCD calculations were compared to the measurements.

2 Data selection and MC simulations

The data were collected with the ATLAS detector during 2010, at a centre-of-mass energy of $\sqrt{s} = 7$ TeV. Events were recorded using a single-photon trigger, with a nominal transverse energy threshold of 40 GeV. This trigger has an efficiency for photons with $E_T^\gamma > 45$ GeV and $|\eta^\gamma| < 2.37$ close to 100%. The total integrated luminosity of the collected sample amounts to 37.1 ± 1.3 pb^{-1}.

Events were required to have a reconstructed primary vertex, with at least five associated tracks with $p_T^{\rm track} > 150$ MeV, consistent with the average beam-spot position.

The photon-candidate selection is based on the reconstruction of isolated electromagnetic clusters in the calorimeter. Clusters without matching tracks were classified as unconverted photons, whereas clusters matched to tracks were classified as converted photon candidates. The photon candidate was required to be isolated by restricting the

[a] e-mail: josu.cantero@cern.ch

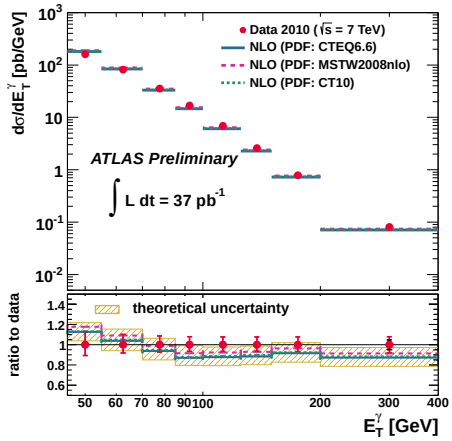

Figure 1. The measured differential cross section for isolated-photon plus jet production (dots) as a function of E_T^γ [11].

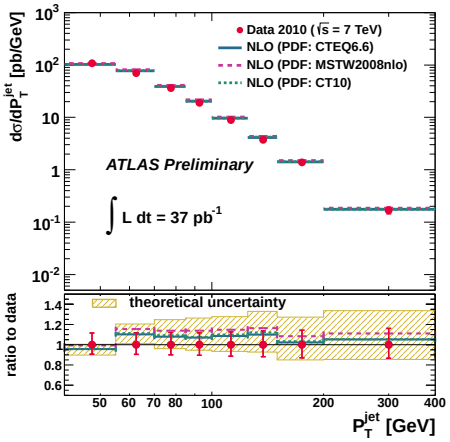

Figure 2. The measured differential cross section for isolated-photon plus jet production (dots) as a function of $P_T^{\rm jet}$ [11].

amount of transverse energy around its direction ($E_{T,\rm det}^{\rm iso}$). The measured value of $E_{T,\rm det}^{\rm iso}$ was corrected by subtracting the estimated contributions from the underlying event and additional inelastic pp interactions [6]. After all these corrections, $E_{T,\rm det}^{\rm iso}$ was required to be below 3 GeV. The relative contribution to the total cross section from fragmentation processes decreases after the applications of these requirements, though it remains non-negligible especially at low transverse energies.

Jets were reconstructed from three-dimensional topological clusters built from calorimeter cells, using the anti-k_t algorithm with distance parameter $R = 0.6$. The jet four-momenta were computed from the sum of the jet constituent four-momenta, treating each as a four-vector with zero mass and then recalibrated using a jet energy-scale (JES) correction. Jets overlapping with the candidate photon or with an isolated electron were not considered. The requirement on the electrons suppresses contamination from W/Z plus jet events.

The MC programs Pythia 6.423 [7] and Herwig 6.510 [8] were used to generate the signal events. The event-generator parameters, including those of the underlying-event modelling, were set according to the AMBT1 [9] and AUET1 [10] tunes for Pythia and Herwig, respectively.

Particle-level jets in the MC simulations were identified using the anti-k_t jet algorithm and built from stable particles ($\tau > 10$ ps). The measured differential cross sections refer to particle-level jets and photons which are isolated by requiring $E_{T,\rm part}^{\rm iso} < 4$ GeV in a cone of radius $R = 0.4$.

3 Backgrund subtraction, signal-yield estimation and cross-section measurement procedure

A non-negligible background contribution remains in the selected sample. This background comes predominantly from QCD processes in which a jet is misidentified as a photon. A background subtraction method was devised which does not rely on MC background samples and uses instead signal-depleted control regions. The background

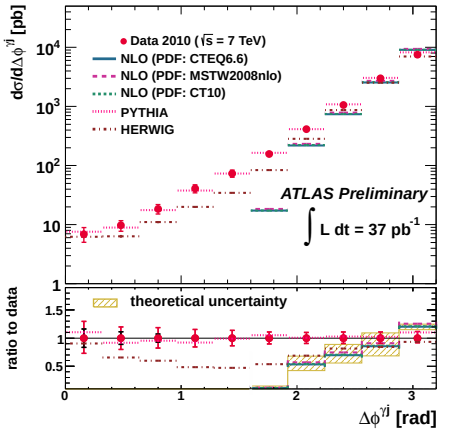

Figure 3. The measured differential cross section for isolated-photon plus jet production (dots) as a function of $\Delta\phi^{\gamma j}$ [11].

contamination in the selected sample was estimated using the same two-dimensional sideband technique as in the previous analyses [6] and then subtracted bin-by-bin from the observed yield.

The data distributions, after background subtraction, were corrected to the particle level using a bin-by-bin correction procedure. For this approach to be valid, the uncorrected distributions of data must be adequately described by the MC simulations at the detector level. This condition was satisfied by both the Pythia and Herwig MC samples after adjusting the relative fractions of the LO direct-photon and fragmentation components [11].

4 Systematic uncertainties

Several systematic sources that affect the measurements were considered [11]. In the following the most important systematic sources are listed. Average values, expressed in percent and shown in parentheses, quantify their effects on the cross section as a function of $|\cos\theta^{\gamma j}|$:

- simulation of the detector geometry. This systematic accounts for the uncertainties originated from the limited

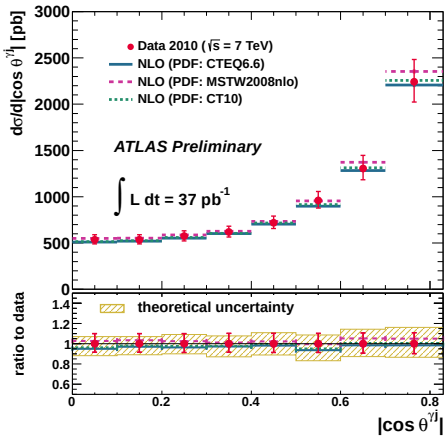

Figure 4. The measured differential cross section for isolated-photon plus jet production (dots) as a function of $|\cos\theta^{\gamma j}|$ [11].

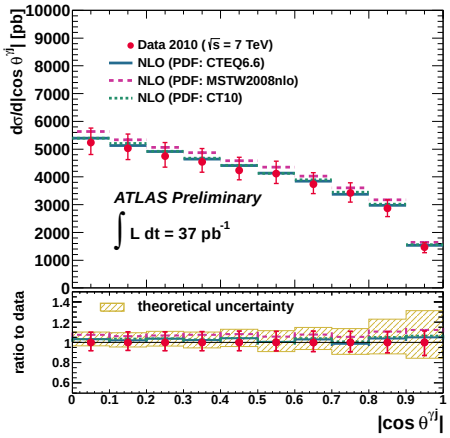

Figure 5. The measured differential cross section for isolated-photon plus jet production (dots) as a function of $|\cos\theta^{\gamma j}|$ without the cuts on $M^{\gamma j}$ and $|\eta^{\gamma} + y^{\rm jet}|$ [11].

knowledge of the material in the detector. This affects in particular the photon-conversion rate and the development of electromagnetic showers (±5%);

- jet and photon energy scale. Differences between the energy scale in data and simulations lead to systematic uncertainties. (photon energy scale: ±1%; jet energy scale: ±5%);
- uncertainty arising from the experimental isolation requirement (+4%).

5 Next-to-leading-order QCD calculations

The NLO QCD calculations used in the analysis presented here were computed using the program JETPHOX [12]. The number of flavours was set to five. The renormalisation (μ_R), factorisation (μ_F) and fragmentation (μ_f) scales were chosen to be $\mu_R = \mu_F = \mu_f = E_T^{\gamma}$. The calculations were performed using the CTEQ6.6 [13] parametrisations of the proton PDFs and the NLO photon BFG set II photon fragmentation function [14]. The strong coupling constant was calculated at two loops with $\alpha_s(M_Z) = 0.118$.

The NLO QCD predictions were corrected to the particle level by applying a multiplicative factor calculated from MC models. The following sources of uncertainty in the theoretical predictions were considered: higher orders (±14%); proton PDF (±3.5%); value of $\alpha_s(M_Z)$ (±2.5%) and the modelling of the QCD cascade, hadronisation and underlying event (±0.5%).

6 Results

The predictions of the NLO QCD calculations are compared to the data in Figs. 1 to 5. The predictions give a good description of the E_T^{γ} and $P_T^{\rm jet}$ measured cross sections. The NLO QCD calculation fails to describe the measured $\Delta\phi^{\gamma j}$ distribution, as expected due to the fact that in the NLO QCD calculation, the photon and the leading jet cannot be in the same hemisphere in the transverse plane, i.e. $\Delta\phi^{\gamma j} \geq \pi/2$. The leading-logarithm parton-shower prediction of PYTHIA gives a good description of the data in the whole range measured whereas HERWIG fails to describe the data (see Fig. 3). The measured cross sections as functions of $|\cos\theta^{\gamma j}|$ are described well by the NLO QCD calculations.

References

[1] T. Pietrycki and A. Szczurek, Phys. Rev. **D 76,** 034003 (2007).
[2] Z. Belghobsi et al., Phys. Rev. **D 79,** 114024 (2009).
[3] M. Cacciari, G.P. Salam and G. Soyez, JHEP **0804,** 063 (2008).
[4] ATLAS Collaboration, Phys. Lett. **B 716,** 1 (2012).
[5] CMS Collaboration, Phys. Lett. **B 716,** 20 (2012).
[6] ATLAS Collaboration, Phys. Rev. **D 83,** 052005 (2011).
[7] T. Sjöstrand, S. Mrenna and P.Z. Skands, JHEP **0605,** 026 (2006).
[8] G. Corcella et al., JHEP **0101,** 010 (2001).
[9] ATLAS Collaboration, ATLAS-CONF-2010-031.
[10] ATLAS Collaboration, ATL-PHYS-PUB-2010-014.
[11] ATLAS Collaboration, ATLAS-CONF-2013-023.
[12] S. Catani et al., JHEP **0205,** 028 (2002).
[13] P. Nadolsky et al., Phys. Rev. **D 78,** 013004 (2008).
[14] L. Bourhis, M. Fontannaz and J. Ph. Guillet, Eur. Phys. J. **C 2,** 529 (1998).